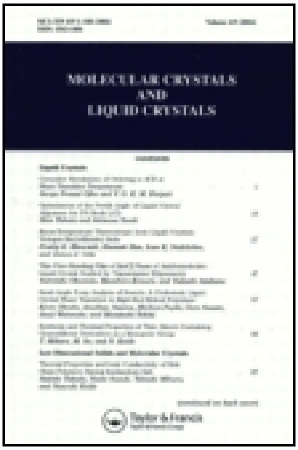

Molecular Crystals and Liquid Crystals
Publication details, including instructions for authors and subscription information:
http://www.tandfonline.com/loi/gmcl18

Refractive Indices of a Methylstilbene Polymer Liquid Crystal

N. A. Vaz [a] , G. W. Smith [a] , G. P. Montgomery JR. [a] , W. D. Marion [a] , V. Percec [b] & M. Lee [b]

[a] Physics Department, General Motors Research Laboratories, Warren, MI, 48090-9055

[b] Department of Macromolecular Science, Case Western Reserve University, Cleveland, Ohio, 441 06-2699

Version of record first published: 24 Sep 2006.

To cite this article: N. A. Vaz , G. W. Smith , G. P. Montgomery JR. , W. D. Marion , V. Percec & M. Lee (1991): Refractive Indices of a Methylstilbene Polymer Liquid Crystal, Molecular Crystals and Liquid Crystals, 198:1, 305-321

To link to this article: http://dx.doi.org/10.1080/00268949108033407

Mol. Cryst. Liq. Cryst., 1991, Vol. 198, pp. 305–321
Reprints available directly from the publisher
Photocopying permitted by license only

Printed in the United States of America

Refractive Indices of a Methylstilbene Polymer Liquid Crystal

N. A. VAZ, G. W. SMITH, G. P. MONTGOMERY, JR.
and W. D. MARION

Physics Department, General Motors Research Laboratories, Warren, MI 48090-9055

and

V. PERCEC and M. LEE

Department of Macromolecular Science, Case Western Reserve University, Cleveland, Ohio, 44106-2699

(Received July 25, 1990)

The refractive indices of a side-chain polymer liquid crystal, 4-ω-hydroxyhexyl-1-oxy-)-4′-methoxy-α-methylstilbene, polymethacrylate with weight-averaged molecular weight $\bar{M}_w = 54{,}000$ have been measured as a function of temperature using a Jelley-Leitz refractometer. In these measurements the polymer was aligned by shear flow in the nematic phase. We developed a model for this alignment in order to interpret the data in terms of the polarization direction of the refracted light. The results suggest that the polymer is aligned so that one of its minor optical axes (i.e., one of the directions along which one measures the ordinary refractive index) lies along the flow direction and its principal optical axis (i.e., the direction along which one measures the extraordinary refractive index) is distributed in a plane perpendicular to the flow axis.

Keywords: refractive index, polymer liquid crystal, birefringence, methylstilbene, nematic polymer

1. INTRODUCTION

Polymer liquid crystals (P-LCs) are materials which offer a unique combination of properties of both polymers and liquid crystals. For example, P-LCs have the low density of a polymer; on the other hand, P-LCs respond to applied electric and magnetic fields and even shear forces in a manner similar to liquid crystals.

The first P-LCs were polyesters synthesized by Roviello and Sirigu in 1975.[1] Morgan[2] subsequently synthesized some polyazomethines and, since then, a vast number of materials has been prepared.[3–6] All these materials were main chain P-LCs (MC-P-LCs). That is, the polymers were characterized by a main chain whose segments aligned parallel to each other or to segments of other chains. In 1978 Finkelman *et al.* synthesized the first side-chain polymer liquid crystals (SC-P-LCs).[7] In SC-P-LCs the liquid crystalline properties arise from side groups attached to the main chain, so that there is some decoupling of the polymeric properties from the liquid crystalline behavior.[8]

Many optical and mechanical properties of MC-P-LCs have been measured. However, few parameters characterizing SC-P-LCs have been measured. One goal of the present work was to perform the first measurements of the refractive indices of a SC-P-LC over a wide temperature range. In order to consistently interpret the measured values we had to develop a model for the flow-alignment of the polymer. Before we describe our measurements and the model, we discuss the practical importance of measuring the temperature dependence of the optical properties of a SC-P-LC.

Recently, it has been proposed[9,10] that PDLC films (i.e., polymer-dispersed liquid crystal films) which can electrically switch light transmittance[11-17] might be prepared using SC-P-LCs in conjunction with low molecular weight liquid crystals (LMW-LCs) in order to reduce both haze and variation of transmittance with temperature. These problems, which have been observed in electro-optic devices incorporating such films,[11,18-22] are due to a mismatch of the refractive indices of the liquid crystal and the polymer matrix.

In fact, because the LMW-LC is birefringent (i.e., characterized by two refractive indices) while the polymer matrix is isotropic (i.e., characterized by a single refractive index), a perfect refractive index a match cannot be obtained for all angles of observation in any given situation. Moreover, because the temperature dependence of the polymer refractive index is usually quite different from that of one or both refractive indices of the LMW-LC,[23] the mismatch can be large and strongly temperature-dependent. As a result, haze and/or a variation of transmittance with temperature will be observed.

Thus, it has been proposed[9,10] that if a LMW-LC were dispersed in a high molecular weight liquid crystal (HMW-LC) or, in other words, a P-LC, one might be able to match their refractive indices not only along many directions of observation but also over a wide range of temperatures. This concept assumes that both materials have similar values of refractive indices and similar rates of change of those indices with temperature. Thus, another goal of the present work was to determine whether the measured values of the refractive indices of a SC-P-LC do indeed show the hoped-for similarity to values typical for LMW-LCs.

In the next sections we report values measured over a wide range of temperatures for the refractive indices of a SC-P-LC methylstilbene methacrylate, 4-(ω-hydroxyhexyl-1-oxy-)-4′-methoxy-α-methylstilbene, polymethacrylate, with weight-averaged molecular weight $\bar{M}_w = 54{,}000$, aligned by shear flow. Values were measured for two orthogonal directions of the light polarization. We then present a model for the alignment of the polymer under the shear flow which allowed us to relate these measured values to the polymer's ordinary and extraordinary refractive indices.

2. MATERIALS

We investigated the refractive indices of the methylstilbene methacrylate P-LC and, for purposes of comparison, we also measured the refractive index of its monomer.

The materials were prepared as described in Reference 24. The intermediary alcohol 4-(ω-hydroxyhexanyl-1-oxy-)-4′-methoxy-α-methylstilbene, CAS Registry No. 109888-76-8 or, for short, (4′-6-OH), was first prepared and converted to the monomer, methacrylic acid, -4-(ω-hydroxyhexyl-1-oxy-)-4′-methoxy-α-methylstilbene, CAS Registry No. 109835-54-3 or, for short, (4′-6-MA), by esterification with methacrylol alcohol.

The methylstilbene polymethacrylate, -4-(ω-hydroxyhexyl-1-oxy-)-4′-methoxy-α-methylstilbene, polymethacrylate, CAS Registry No. 118400-12-7 or, for short, (4′-6-PMA), was prepared by radical polymerization of the monomer in dry benzene using AIBN as initiator at 60°C for 20 hours and purified by successive reprecipitations from tetrahydrofuran (THF) solution in acetone and methanol until gel permeation chromatography (GPC) curves showed no traces of unreacted monomer or oligomers. The chemical structure of (4′-6-PMA) is illustrated in Figure 1.

The thermal transitions of the monomer and polymer were determined using a Perkin-Elmer DSC-2 calorimeter using methods described previously.[13,14] Samples weighing approximately 5 mg were hermetically sealed in aluminum pans, placed in the calorimeter sample holder, and cooled to 190 K (− 83°C). After equilibration the temperature was programmed linearly (at 20 K/min) over the range of interest while the sample's rate of heat absorption was recorded. Figure 2 is a resulting DSC thermogram for a sample of methylstilbene SC-P-LC.

Two phase change regions are apparent: a change in baseline at the glass transition and an endothermic peak at the nematic-isotropic transition. The glass transition temperature, T_g, is conventionally taken to be the temperature at which the DSC curve is half-way between extrapolated tangents to the baselines above and below the transition region. The nematic-isotropic transition temperature, T_{ni}, can be defined in several ways: (i) the temperature of the peak maximum (useful for

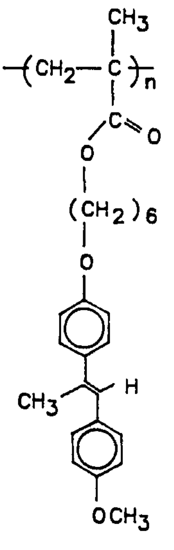

FIGURE 1 Illustration of the chemical structure of the methylstilbene polymer liquid crystal (4′-6-PMA).

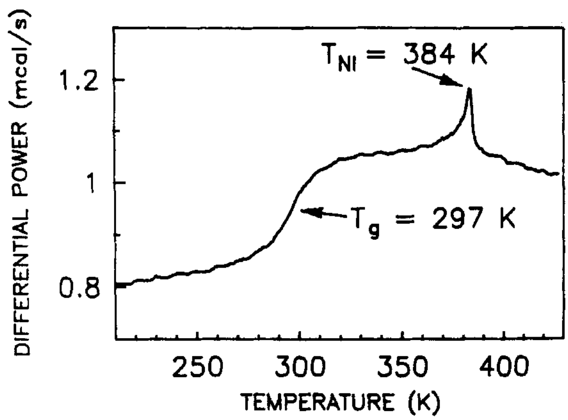

FIGURE 2 DSC thermal scan for the methylstilbene polymer (4′-6-PMA). Endothermic transitions are upward going. Both glass and nematic-isotropic transitions are apparent.

broad transitions like the present one), (ii) the temperature at which a tangent to the steepest portion of the peak's leading edge strikes the point at which the DSC curve first departs from the baseline (slightly dependent on baseline determination), and (iii) the point at which the DSC curve first departs from the baseline (very sensitive to baseline choice). For the sample of Figure 2, definition (i) yields T_{ni} = 385 K (112°C), definition (ii) a value about 379 K (106°C), and definition (iii) an approximate value of 364 K (91°C). It will be seen below that definitions (i) and (ii) give somewhat higher values than those from our refractive index studies. The difference is attributable to several factors: the inherent differences of each method in defining the transition, some experimental uncertainty in the temperature determined in the index measurement, and the possibility that some sample degradation occurred during the index measurement (the samples for that study could, of course, not be sealed). We plan to resolve the difference between the two sets of results by precision thermal microscopy. The nematic-isotropic transition enthalpy, ΔH_{ni}, was determined from the area of the endothermic peak, as calculated by the calorimeter data station. The resulting magnitude of ΔH_{ni} is also sensitive to the choice of baseline.

Our calorimetric studies yielded the following values for the transition parameters of the methylstilbene SC-P-LC (as determined from initial DSC heating scans of several samples): $T_g = 303 \pm 2$ K (30°C); $T_{ni} = 385 \pm 1$ K (112°C); $\Delta H_{ni} = 0.69 \pm 0.1$ cal/g (0.28 K cal per monomer repeat unit). (A small amount of hysteresis was also observed, with lower values of T_g, T_{ni}, and ΔH_{ni} obtained from cooling scans.) Subsequent DSC scans resulted in appreciable decreases in all three quantities, indicating that some sample decomposition occurs at elevated temperatures. For example, a sample heated to 500 K (227°C) exhibited a 50% decrease of ΔH_{ni}, a 30 K depression of T_{ni}, but only a 6 K decrease in T_g. Smaller decreases were observed for repeated scans to temperatures a few decades above T_{ni}. Clearly, more stable polymer liquid crystals will have to be found for practical applications.

The molecular weight of the polymer was determined by GPC with a Perkin-

Elmer Series 10 LC instrument equipped with LC-100 column oven, LC-600 autosampler, and Sigma 15 data station.

Finally, using a Carl-Zeiss optical polarizing microscope (magnification: 100×) equipped with a Mettler FP 82 hot stage and a Mettler FP 800 central processor, the liquid crystalline phase of the methylstilbene methacrylate polymer was identified by its texture as a nematic phase extending from T_g to T_{ni}.

3. REFRACTIVE INDEX MEASUREMENTS

3.1 The Jelley-Leitz Refractometer

The refractive indices were measured using a Jelley-Leitz refractometer[25] equipped with a heating stage to measure refractive indices from room temperature to about 200°C. All measurements were done near the mean sodium D line wavelength (589.3 nm) using an interference filter with a narrow band centered at 589.6 nm to filter the light from a standard incandescent light bulb.

This instrument has been used to measure the refractive indices of polymeric materials, including epoxies[23] and ultraviolet curable adhesives. Figure 3 is a schematic illustration of the construction of the instrument. We will now review its principle of operation.

The basic principle of the refractometer involves the measurement of the relative

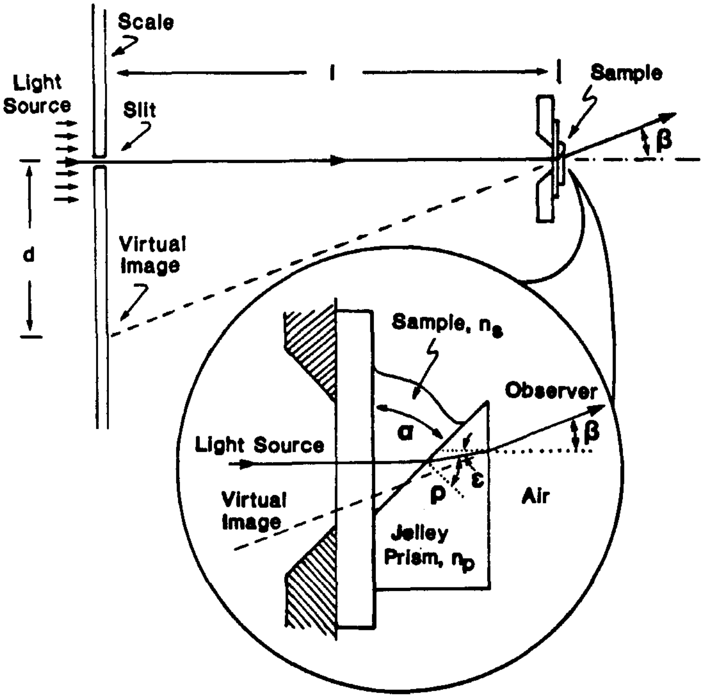

FIGURE 3 Schematic illustration of the Jelley-Leitz refractometer.

displacement of the virtual image and the real image of a point source. The displacement is due to refraction of light rays at the interface between the sample of unknown index n_s and a prism (Jelley prism) of known index n_P and angle α. As Figure 3 illustrates, a second refraction takes place at the interface between the Jelley prism and air ($n_0 = 1$). Applying Snell's Law to these interfaces gives:

$$n_s \sin \alpha = n_P \sin \rho,$$

$$n_P \sin \varepsilon = n_0 \sin \beta. \tag{1}$$

The geometry of the problem provides the supplementary relation:

$$\varepsilon = \rho - \alpha. \tag{2}$$

Solving these equations for n_s we get:

$$n_s = \sqrt{n_P^2 - c^2} + c, \tag{3}$$

where

$$c = \sin \beta = d/\sqrt{d^2 + l^2} \tag{4}$$

is an experimentally measured quantity, d and l are defined in Figure 3, and the prism angle and refractive index are, respectively, $\alpha = 45°$ and $n_P = 1.515$. A scale in the refractometer allows direct readout of the refractive index.

Finally, a calibration of the instrument at various temperatures established the experimental error in the refractive index at ± 0.003.

Using this technique we measured n_{mono}, the refractive index of the monomer (4′-6-MA) above its melting temperature $T_m = 53$°C (in agreement with the value determined from DSC), and n_i the refractive index of the P-LC (4′-6-PMA) in its isotropic phase, above $T_{ni} = 101$°C (a somewhat smaller value than that determined from DSC). The refractive indices were measured to temperatures as high as about 150°C.

3.2 Sample Alignment

In order to measure both the ordinary and extraordinary refractive indices of a liquid crystalline material the sample has to be well aligned with its nematic axis of symmetry parallel to the wedge of the Jelley prism (perpendicular to the plane of Figure 3). For low molecular weight liquid crystals, a polyimide surface treatment was applied to both the Jelley prism and glass slide and then buffed in a direction parallel to the wedge to produce the desired alignment.[26,27]

Unfortunately, the buffed polyimide layer did not produce sufficient aligning force to induce bulk alignment of the methylstilbene methacrylate polymer. Consequently, we tried to induce the polymer alignment via shear forces. We found that, by shearing the Jelley prism over the glass slide in a direction parallel to the prism's wedge, we would observe two distinct refracted lines after heating the polymer into its nematic phase, near T_{ni}. These two refracted lines would then persist while heating or cooling the sample. They would be lost below the glass phase transition or above the nematic-isotropic phase transition, but could be recovered at any time by heating the sample to its nematic phase, preferably near T_{ni}.

Using this alignment technique we measured two refractive indices for the methylstilbene polymer (4'-6-PMA) between $T_g = 32°\text{C}$ and $T_{ni} = 101°\text{C}$. We note that the glass transition temperature determined from these optical experiments agrees well with the value determined from DSC. In the next sections we will discuss how these measured values relate to the ordinary and extraordinary refractive indices of the polymer.

4. RESULTS

4.1 Refractive Index of Monomer (4'-6-MA)

The refractive index of the monomer (4'-6-MA), n_{mono}, was measured from its melting temperature $T_m = 53°\text{C}$ to about 150°C (see Figure 3, dashed squares). The data were least squares fitted to a straight line (solid line in Figure 3 drawn through the dashed squares), giving a value of $(dn/dT)_{T_0} = -4.3156 \times 10^{-4}°\text{C}^{-1}$ for the coefficient of temperature dependence of the refractive index at $T_0 = 25°\text{C}$. This value compares well with those measured for the refractive indices of other monomers,[23,26,27] which typically fall in the range[28] $-4.5 \times 10^{-4}°\text{C}^{-1} \leq (dn/dt)_{T_0} \leq -2.4 \times 10^{-4}°\text{C}^{-1}$.

4.2 Refractive Index of Polymer (4'-6-PMA)

4.2.1 Isotropic Phase of Polymer (4'-6-PMA). The refractive index of the methylstilbene polymer liquid crystal (4'-6-PMA) in its isotropic phase, n_i, was measured above $T_{ni} = 101°\text{C}$ up to near 150°C (see Figure 3, squares). The data were least squares fitted to a straight line (solid line in Figure 3 drawn through the squares), giving a value of $(dn/dT)_{T_0} = -4.6667 \times 10^{-4}°\text{C}^{-1}$ for the coefficient of temperature dependence of the refractive index. This value compares well with those of other liquid crystals in the isotropic phase.[23,26,27] It is also very similar to the value obtained for the monomer (see *4.1*).

4.2.2 Nematic Phase of Polymer (4'-6-PMA). Two sharp and distinct lines were observed in the Jelley-Leitz refractometer in the nematic phase of the methylstilbene polymer liquid crystal aligned under shear flow. They correspond to two orthogonal directions of polarization of light. Using two linear polarizers and a variable-phase optical retarder, we found that these lines were essentially linearly polarized. The line corresponding to the *lower* value of the refractive index was polarized in a direction *parallel* to the prism's wedge, and the line corresponding to the *higher* value of the refractive index was polarized in the direction *perpendicular* to the prism's wedge. We will refer to these two experimental values as $n_{\parallel}$ and $n_{\perp}$, respectively.

The data were recorded from T_g to T_{ni}. Figure 4 shows $n_{\parallel}$ measured in the heating and cooling cycles and $n_{\perp}$ measured only in the heating cycle. The agreement between the data recorded in the heating and cooling cycles illustrates the absence of significant hysteresis of the data with temperature. The data shown at the two lowest temperatures were recorded either in a supercooled nematic phase or within the glass phase (which would have retained the alignment from the nematic phase).

In order to interpret the experimental values $n_{\parallel}$ and $n_{\perp}$ in terms of n_o and n_e, respectively the ordinary and the extraordinary refractive indices of the polymer, we developed a model for the flow-induced alignment of the polymer.

5. DISCUSSION

We will discuss two different models for the flow-induced alignment of the polymer and show that only the second model is consistent with all the experimental evidence.

5.1 Model 1

Since the measured values of the refractive index correspond to two orthogonal directions of polarization of linearly polarized light, in this first model we assume that the polymer was aligned by the shear flow such that $n_{\perp} = n_e$ and $n_{\parallel} = n_o$.

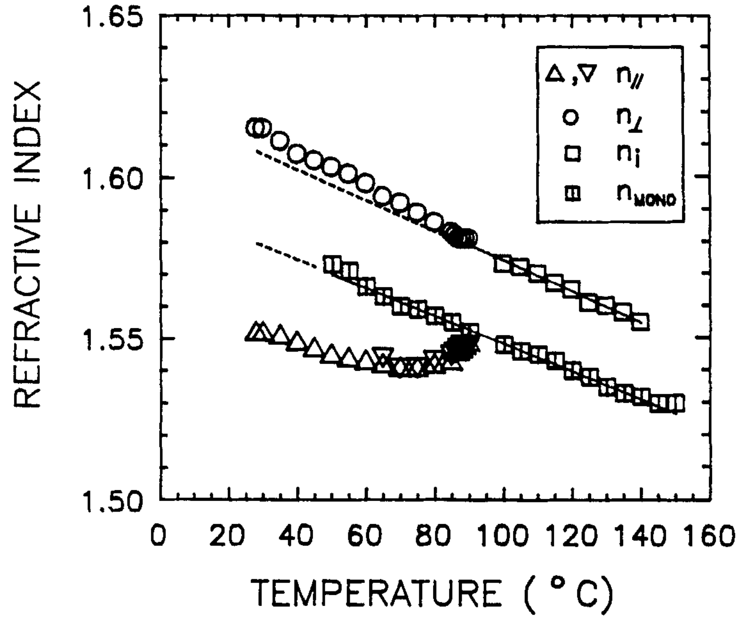

FIGURE 4 Refractive indices of the methylstilbene monomer (4′-6-MA): dashed squares, and of its polymer, (4′-6-PMA): squares, triangles and circles, respectively n_i, $n_{\parallel}$ and $n_{\perp}$. The solid lines are least squares fit to the data, and the dashed lines their extrapolations.

This is what one would expect by analogy with low molecular weight liquid crystals because they typically have positive birefringence (i.e., $\Delta n = n_e - n_o > 0$).[29,30]

This model has the following difficulty. Considerable experimental evidence in the literature[29-33] shows that the *isotropic* average of the refractive indices of a nematic liquid crystalline material,[34]

$$\bar{n}_{oe}^{iso} = (2n_o + n_e)/3, \qquad (5)$$

gives values which are comparable to the isotopic refractive index values of the same material extrapolated into the liquid crystalline phase to the same temperature.[35]

Thus, with reference to Figure 5, the experimental evidence[29-33] would predict that the average values $\bar{n}_{oe}^{iso} = \bar{n}_{\parallel\perp}^{iso}$ (see Figure 5) should fall near the extrapolated values from the isotropic refractive index. These extrapolated values are shown in the same figure by the dashed line which is an extension of the solid line that was least squares fitted to the data from the isotropic phase. Clearly, this prediction is incorrect and, in consequence, we abandoned this model.

However, before describing the second model, we point out that the first model has one additional difficulty. If the analogy with low molecular weight liquid crystals were to be considered further, then the molecular arrangement which one would expect from a nematic under shear flow in the gap between the prism and the glass slide would be such that the nematic axis of symmetry would lie in a plane parallel

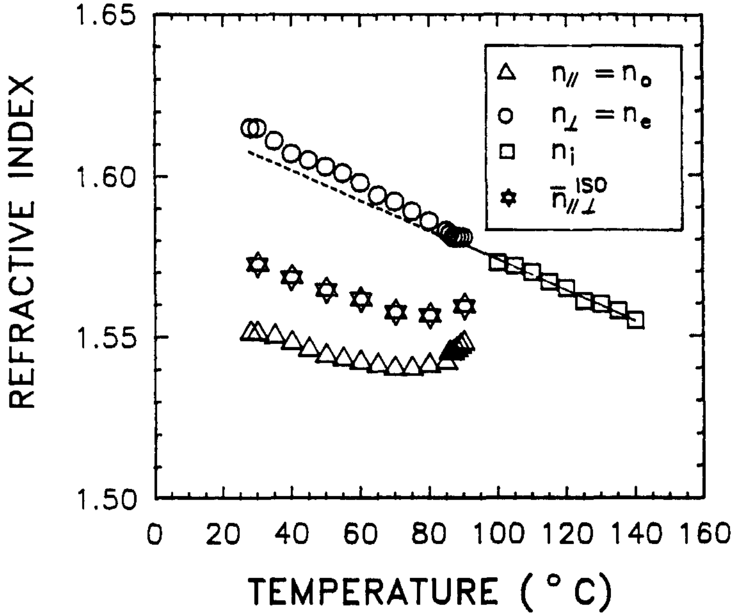

FIGURE 5 Refractive indices of the methylstilbene polymer (4′-6-PMA): isotropic phase (squares); $n_\parallel$ (triangles); $n_\perp$ (circles); *isotropic* average of $n_\parallel$ and $n_\perp$, $\bar{n}_{\parallel\perp}^{iso}$, calculated according to *Model 1* assuming that $n_\parallel = n_o$ and $n_\perp = n_e$ (stars); least squares fit to the isotropic data (solid line) and its extrapolation to the nematic (dashed line). Note the discrepancy between $\bar{n}_{\parallel\perp}^{iso}$ and the dashed line.

to the wedge of the Jelley' prism.[29,30,36–38] This would imply that the largest of the measured refractive index values should correspond to a direction of polarization parallel to the prism's wedge, in disagreement with the experimental observation (see *4.2.2*).

5.2 Model 2

In order to be consistent with the experimental observations that (i) the two measured values of the refractive index correspond to two orthogonal directions of polarization of light and (ii) the light polarization is linear, we will assume that one of the measured values corresponds to one of the principal refractive indices of the material, n_o or n_e, and the other value is the result of an average on a plane of the side-chain polarizabilities which contribute to those values. That is, either $n_\parallel$ corresponds to n_o or n_e and $n_\perp$ is some average of local values of n_o and n_e, or $n_\perp$ corresponds to n_o or n_e and $n_\parallel$ is the averaged value.

Strictly speaking, this average is to be understood as the average of the local polarizabilities contributing to the birefringence of the sample and not as an average from different regions of the sample oriented at different angles. The latter case would result in refraction of light at various directions, and we would then observe a wide distribution of light in the refractometer corresponding to all angles of refraction between those that give rise to n_o and n_e. Since the observed lines are sharp, the orientation of the sample is well established and the average takes place at a local level. However, for simplicity of the presentation, we will refer to the average as an average of refractive indices.

If we assume that the birefringence is positive, then $n_\parallel = n_o$. One corollary to the last statement is that the shear-flow alignment of the polymer leads to an orientation of the symmetry axis of the nematic phase which is not in a plane parallel to the prism's wedge. However, in a SC-P-LC the competition between the influence of flow on the main chain and that of the liquid crystalline side chain could produce an alignment different from that expected for a LMW-LC.[36–38]

At this point it is not possible to provide a detailed description of the configuration of the SC-P-LC on which to base our optical model. That is, even though it may be justified to assume that the main contribution to the measured birefringence is due to the liquid crystalline side chains, an attempt to visualize the configuration of the main chain and/or of the side chains would be speculative.

In *Model 2*, we let

$$\begin{aligned} n_\parallel &= n_o, \\ n_\perp &= \overline{n}_{oe}^{cyl,a}, \end{aligned} \tag{6}$$

where we used the following notation: the superscript *cyl*, *a* means that the *averaged* value $\overline{n}$ is calculated from a cylindrical or planar average of refractive indices distributed on a plane perpendicular to the Jelley prism's wedge with a mean orientation centered at the angle a measured from the XY-plane. Figure 6 shows the local coordinate axes $(x'y'z')$ associated with the optic axes of the sample and

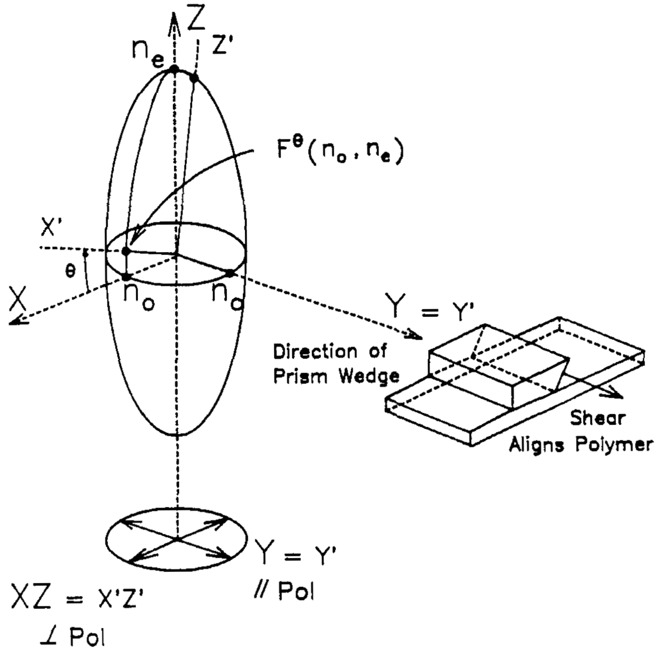

FIGURE 6 Coordinate axes ($x'y'z'$) defining the orientations of the optic axes of the sample with respect to the (XYZ) axes defining the orientation of the Jelley prism.

their relative orientation with respect to the Jelley prism and glass slide which are on the XY-plane of the laboratory coordinate frame (XYZ).

If the sample were aligned such that the frames ($x'y'z'$) and (XYZ) coincided, one would measure $n_\parallel = n_\perp = n_o$. However, because the experimental values for $n_\perp$ differ from n_o, we let the sample have a distribution of the optic axes such that $n_\perp$ becomes an average of n_o and n_e taken on a plane. In other words, on a plane perpendicular to the wedge of the Jelley prism, the contributions to the sample's polarizability will be oriented at various angles θ (see Figure 6), so that the sample will present an effective refractive index

$$n_\perp = \bar{n}_{oe}^{cyl,a} = \frac{1}{\pi}\int_0^\pi F^\theta(n_o, n_e)P(\theta + a)\,d\theta, \tag{7}$$

with

$$F^\theta(n_o, n_e) = \frac{n_o n_e}{\sqrt{n_e^2 \cos^2\theta + n_o^2 \sin^2\theta}}, \tag{8}$$

where $P(\theta)$ is the probability distribution function of finding each angle θ, and the angle a is the mean value of the optic axis distribution: $a \neq 0$ means that the z'-axis may be preferentially oriented at that angle.

Because the symmetry of the sample is that of a nematic liquid crystal, the symmetry must be described by a second order Legendre polynomial,[29]

$$P_2(\cos\theta) = (3\cos^2\theta - 1)/2. \tag{9}$$

The simplest form for the probability distribution function, $P(\theta)$ is then:

$$P(\theta) = 2\cos^2\theta, \tag{10}$$

which is normalized so that

$$\frac{1}{\pi}\int_0^{\pi} P(\theta)d\theta = 1. \tag{11}$$

Letting $\Delta = 2\cos^2 a$ and defining $F(k, \pi/2)$ and $E(k, \pi/2)$ as the complete elliptical integrals of first and second kind, respectively, with modulus k defined by:

$$k = \frac{n_e^2 - n_o^2}{n_e^2}, \tag{12}$$

we can write:[39]

$$n_\perp = \frac{2}{\pi} n_o\{\Delta F(k, \pi/2) + (1 - \Delta)[F(k, \pi/2) - E(k, \pi/2)]\}, \tag{13}$$

or, expanding in a power series in k:

$$n_\perp = \bar{n}_{oe}^{cyl,a} = \left[1 + \frac{3 - \Delta}{8}k^2 + \frac{45 - 18\Delta}{192}k^4 + \dots\right]. \tag{14}$$

Equations 12 and 14 can be solved for n_e to give:

$$\begin{aligned} n_e &= n_e^{cyl,a} \\ &= n_o\left(1 - \frac{-(3 - \Delta) + \sqrt{(3 - \Delta)^2 - 12(5 - 2\Delta)(1 - n_\perp/n_o)}}{3(5 - 2\Delta)/4}\right)^{-\frac{1}{2}}. \end{aligned} \tag{15}$$

Using Equation 15 and the experimental values of $n_\perp$ and $n_\parallel = n_o$, we selected some value for the angle a (the only adjusting parameter in the model) in order to obtain values for $n_e = n_e^{cyl,a}$. Then, using n_o and this value of $n_e = n_e^{cyl,a}$, we calculated the *isotropic* average

$$\bar{n}_{oe}^{iso} = (2n_o + n_e^{cyl,a})/3, \tag{16}$$

which we compared at each temperature with refractive index values obtained from extrapolation of the isotropic phase data into the nematic phase at the same temperature. We iterated this procedure varying the selection for the angle *a* until we obtained a good agreement between these two sets of values.

Figure 7a shows the results of these calculations. In this figure we reproduced from Figure 6 the refractive indices of the methylstilbene polymer (4'-6-PMA) within its isotropic phase, n_i, (squares) and nematic phase, $n_\parallel$ (triangles) and $n_\perp$ (circles). The calculated values shown in Figure 7a are:

1) The *cylindrical* average of $n_\parallel$ and $n_\perp$, $\overline{n}_{oe}^{cyl,a=31.5^\circ}$, calculated according to *Model 2* and assuming that $n_\parallel = n_o$ and $n_\perp = \overline{n}_{oe}^{cyl,a}$ (starred squares); 2) The least squares fit to the isotropic data (solid line) and its extrapolation to the nematic (dashed line); and 3) The *isotropic* average $\overline{n}_{oe}^{iso}$ calculated from $n_o = n_\parallel$ and the calculated values of n_e (dotted line).

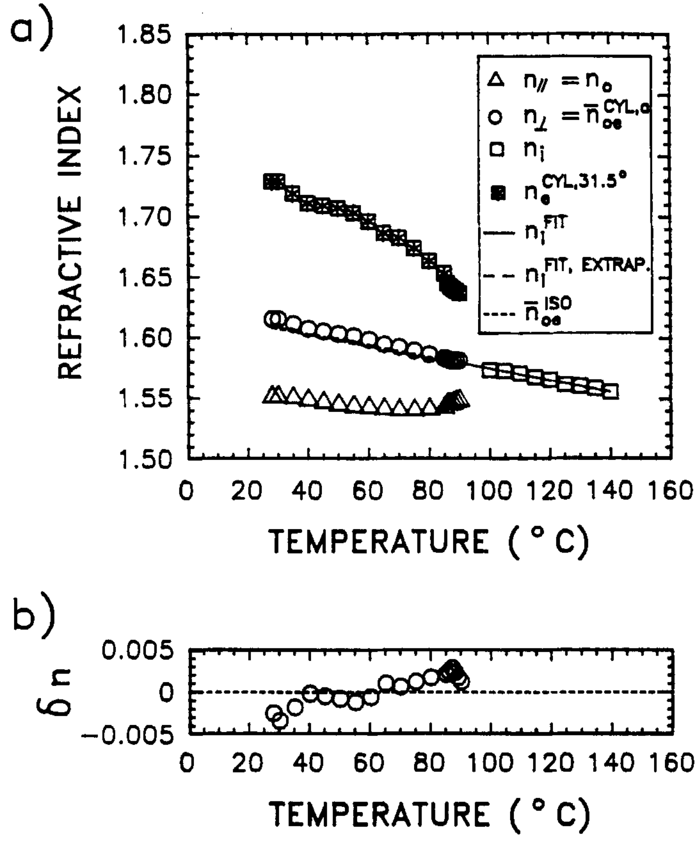

FIGURE 7 a) Refractive indices of the methylstilbene polymer (4'-6-PMA): isotropic phase (squares); $n_\parallel$ (triangles); $n_\perp$ (circles); *cylindrical* average of $n_\parallel$ and $n_\perp$, $\overline{n}_{oe}^{cyl,a=31.5^\circ}$, calculated according to *Model 2* assuming that $n_\parallel = n_o$ and $n_\perp = \overline{n}_{oe}^{cyl,a}$ (starred squares); least squares fit to the isotropic data (solid line) and its extrapolation to the nematic (dashed line); *isotropic* average $\overline{n}_{oe}^{iso}$ calculated from $n_o = n_\parallel$ and the calculated values of n_e (dotted line). Note that the dotted line is nearly superimposed on the dashed line. b) Difference, δn, (circles) between values of the isotropic refractive index extrapolated into the nematic phase and the *isotropic* average $\overline{n}_{oe}^{iso}$ illustrating the good agreement obtained between these two quantities in *Model 2*.

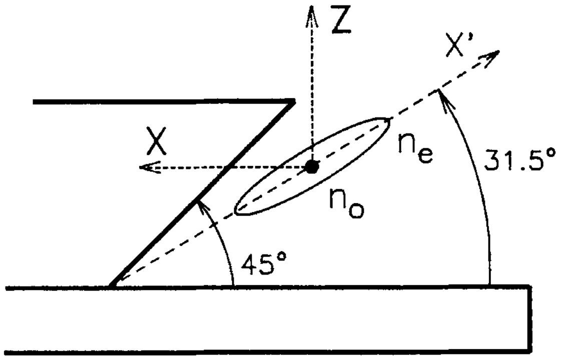

FIGURE 8 Schematic illustration of the Jelley prism and glass slide which confine the sample, and of the calculated orientation for the optic axes of the polymer liquid crystal corresponding to the data plotted in Figure 6 (using *Model 2*).

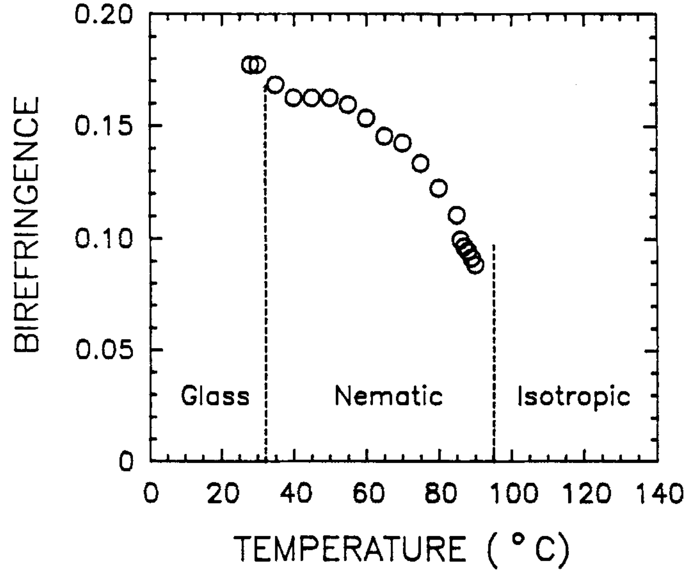

FIGURE 9 Birefringence of the methylstilbene polymer (4'-6-PMA) calculated using *Model 2*.

The value of the only fitting parameter, the angle a, which gave the best agreement is $a = 31.5°$. The quality of the agreement is easily deduced from Figure 7a from the fact that the dotted line is nearly superimposed on the dashed line. The quality of the agreement is also illustrated in Figure 7b where we plotted (circles) the difference,

$$\delta n = n_i^{ext} - \overline{n}_{oe}^{iso}, \tag{17}$$

obtained at each temperature between values of the isotropic refractive index extrapolated into the nematic phase, n_i^{ext}, and the *isotropic* average, $\overline{n}_{oe}^{iso}$.

The fact that best agreement was obtained with for $a = 31.5°$ implies that the orientation imposed on the polymer by the shear flow was such that the principal optic axis of the polymer, i.e., the direction along which one measures n_e, is within the conic section with aperture $\alpha = 45°$ defined by the wedge of the prism (see Figure 7). Although we cannot rule out the solution corresponding to an angle $\pi - a$, the orientation illustrated in Figure 7 for the ellipsoid of refractive index appears reasonable.

Finally, in Figure 8 we plotted the birefringence, $\Delta n = n_e^{cyl,31.5°} - n_o$, of the polymer liquid crystal (4′-6-PMA) as a function of temperature which we calculated from *Model 2*. The birefringence is comparable to that of many LMW-LCs and follows similar trends as a function of temperature.[40] It starts at about 0.08 near T_{ni} and increases with decreasing temperature to 0.18 near 25°C. This temperature is just below T_g measured from calorimetry, suggesting that either we supercooled the nematic phase by about 8 degrees, or that the polymer alignment was preserved within the glass phase.

6. CONCLUSIONS

Using a Jelley refractometer equipped with temperature control, we measured two refractive indices corresponding to two orthogonal directions of light polarization from a methylstilbene polymer liquid crystal ($\overline{M}_w = 54{,}000$) aligned by shear flow.

The data were interpreted using a model in which the polymer liquid crystal aligned under the shear flow such that one of the polymer's minor optical axes aligned parallel to the flow direction and the polymer's major optical axis was distributed in the plane perpendicular to the flow direction with a distribution function which can be described by a $\cos^2 \theta$ function. This distribution function was found centered at an angle of 31.5° measured from the glass slide supporting the Jelley prism (see Figure 7).

Moreover, the temperature dependence of the ordinary and extraordinary refractive indices determined for the polymer liquid crystal from the modeled flow-induced alignment is similar to that of low molecular weight liquid crystals (see Figure 6).

Finally, the optical birefringence calculated from the refractive indices determined under the same model-based assumptions is comparable to that of many low molecular weight liquid crystals. It varies from 0.08 near the nematic to isotropic transition temperature, $T_{ni} = 101°C$, to 0.17 near the glass transition temperature, $T_g = 32°C$ (see Figure 8).

It is thus reasonable to expect that PDLC films prepared from microdispersions of LMW-LCs in polymer liquid crystals similar to the methylstilbene liquid crystal investigated in this work could exhibit improved electro-optic response because of a better index match between the polymer matrix and dispersed liquid crystal droplets over many angles and in a wide range of temperatures. However, as demonstrated from our DSC measurements, even though T_{ni} for this material is sufficiently high for many applications (it is above 100°C), the polymer is unstable at temperatures not too far above the nematic-isotropic transition. Therefore, alternative materials having better thermal stability should be considered.

Acknowledgment

We thank Tom VanSteenkiste and Dan Hayden for assistance in the calorimetric work.

References

1. A. Roviello and A. Sirigu, *J. Pol. Sci. Lett. Ed.*, **13**, 455 (1975).
2. P. W. Morgan, Ger. Offen. 2,620,351, U. S. Appl. 576,236, 9 May 1975.
3. *Liquid Crystalline Order in Polymers*, edited by A. Blumstein, Academic, New York, (1978).
4. *Polymer Liquid Crystals*, edited by A. Blumstein, Plenum Press, New York, (1985).
5. *Recent Advances in Liquid Crystalline Polymers*, edited by L. Chapoy, Elsevier, London, (1985).
6. *Polymer Liquid Crystals*, edited by A. Ciferi, W. Krigbaum, and R. Meyer, Academic Press, New York, (1982).
7. M. Happ, H. Ringsdorf and H. Finkelman, Ger. Offen. 2,722,589, 30 November 1978.
8. *Side Chain Liquid Crystalline Polymers*, edited by C. B. McArdle, Chapman, New York, (1989).
9. J. W. Doane, J. L. West, W. Tamura-Lis and J. B. Whitehead, Jr., "Polymer-dispersed liquid crystal films for haze-free wide-angle-view light shutters," Preprints of the First Pacific Polymer Conference, Dec. 12-15, 1989, Maui, Hawaii.
10. J. L. West, L. C. Chien, and W. Tamura-Lis, "Liquid crystalline epoxies for use in polymer dispersed-liquid crystal films," Preprints of the First Pacific Polymer Conference, Dec. 12-15, 1989, Maui, Hawaii.
11. J. W. Doane, N. A. Vaz, B.-G. Wu and S. Žumer, *Appl. Phys. Lett.* **48**, 269 (1986).
12. J. W. Doane, G. Chidichimo, and N. A. Vaz, US Patent 4,688,900 (Aug. 25, 1987).
13. N. A. Vaz, G. W. Smith and G. P. Montgomery, Jr., *Mol. Cryst. Liq. Cryst.* **146**, 17 (1987).
14. N. A. Vaz, G. W. Smith and G. P. Montgomery, Jr., *Mol. Cryst. Liq. Cryst.* **146**, 1 (1987); N. A. Vaz and G. W. Smith, U.S. Patent 4,728,547, March 1, 1988; G. P. Montgomery, Jr., N. A. Vaz, and G. W. Smith, *Proc. SPIE* **958**, 104 (1988).
15. J. L. West, *Mol. Cryst. Liq. Cryst.* **157**, 427 (1988).
16. J. L. Fergason, U.S. Patents No. 4,435,047, March 6 (1984) and No. 4,616,903, October 14 (1986), and *SID Digest of Technical Paper* **16**, 68 (1985).
17. P. S. Drzaic, *J. Appl. Phys.* **60**, 2142 (1986), and *Mol. Cryst. Liq. Cryst.* **154**, 289 (1988).
18. P. van Konynenburg, S. Marsland and J. McCoy, *Proc. SPIE* **823**, 143 (1987).
19. P. van Konynenburg, R. Wipfler, and J. L. Smith, *Proc. SPIE* **1080**, 62 (1989).
20. B.-G. Wu, J. West, and J. W. Doane, *J. Appl. Phys.* **62**, 3925 (1987).
21. J. W. Doane, A. Golemme, J. L. West, J. B. Whitehead, Jr., and B.-G. Wu, *Mol. Cryst. Liq. Cryst.* **165**, 511 (1988).
22. J. B. Whitehead, Jr., S. Žumer, J. W. Doane, and E. Kardelj, *Proc. SPIE* **1080**, 250 (1989).
23. N. A. Vaz and G. P. Montgomery, Jr., *J. Appl. Phys.* **62**, 3161 (1987).
24. V. Percec and D. Tomazos, *Macromol.* **22**, 2062 (1989).
25. Refractometer model No. 13-947 from Fisher Scientific, Pittsburgh, PA.
26. N. A. Vaz, *Proc. SPIE* **1080**, 53 (1989).
27. N. A. Vaz and G. P. Montgomery, Jr., *J. Appl. Phys.* **65**, 5043 (1989).
28. G. P. Montgomery, "Polymer-Dispersed and Encapsulated Liquid Crystal Films," in *Large-Area Chromogenics: Materials and Devices for Transmittance Control*, edited by C. M. Lampert and C. G. Granqvist, to be published by SPIE, The International Society for Optical Engineering.
29. P. G. de Gennes, *The Physics of Liquid Crystals*, Clarendon Press, New York (1974).
30. W. H. de Jeu, *Physical Properties of Liquid Crystalline Materials*, Gordon and Breach, New York (1980).
31. D. Dolphin, Z. Muljiani, J. Cheng, and R. B. Meyer, *J. Chem. Phys.* **58**, 413 (1973).
32. P. Palffy-Muhoray and D. A. Balzarini, *Can. J. Phys.* **59**, 515 (1981).
33. S. Denprayoonwong, P. Limcharoen, O. Phaovibul, and I. M. Tang, *Mol. Cryst. Liq. Cryst.* **69**, 313 (1981).
34. The notation is the following: the bar stands for an averaged value, the superscript *iso* stands for an isotropic average, and the subscript *oe* specifies that the average was calculated using n_o and n_e values.
35. Some authors use the average $\sqrt{(2n_o^2 + n_e^2)/3}$, but this expression usually gives results which are very similar to those calculated from Equation 5. Since our conclusions would have been very similar had we used either one of the averages, we used the simpler linear average in this work.

36. F. M. Leslie, *Q. J. Mech. Appl. Math.* **19**, 357 (1966); *Arch. Rat. Mech. Anal.* **28**, 265 (1967).
37. J. L. Ericksen, in *Liquid Crystals*, vol. 2, pt. 1, pg. 177, edited by G. Brown, Gordon and Breach, New York, (1969).
38. At least in the bulk of the sample.
39. I. S. Gradshetyn and I. M. Ryzhik, *Tables of Integrals, Series, and Products*, Academic Press (1965).
40. H. Kelker and R. Hatz, *Handbook of Liquid Crystals*, Verlag Chemie (1980).